

RESEARCH ARTICLE

Open Access

# Significance of *glioma-associated oncogene homolog 1 (GLI1)* expression in claudin-low breast cancer and crosstalk with the nuclear factor kappa-light-chain-enhancer of activated B cells (NFκB) pathway

Sierra A Colavito<sup>1,2\*</sup>, Mike R Zou<sup>1</sup>, Qin Yan<sup>1</sup>, Don X Nguyen<sup>1</sup> and David F Stern<sup>1</sup>

## Abstract

**Introduction:** The recently identified claudin-low subtype of breast cancer is enriched for cells with stem-like and mesenchymal-like characteristics. This subtype is most often triple-negative (lacking the estrogen and progesterone receptors (ER, PR) as well as lacking epidermal growth factor 2 (*HER2*) amplification) and has a poor prognosis. There are few targeted treatment options available for patients with this highly aggressive type of cancer.

**Methods:** Using a high throughput inhibitor screen, we identified high expression of glioma-associated oncogene homolog 1 (*GLI1*), the effector molecule of the hedgehog (Hh) pathway, as a critical determinant of cell lines that have undergone an epithelial to mesenchymal transition (EMT).

**Results:** High *GLI1* expression is a property of claudin-low cells and tumors and correlates with markers of EMT and breast cancer stem cells. Knockdown of *GLI1* expression in claudin-low cell lines resulted in reduced cell viability, motility, clonogenicity, self-renewal, and reduced tumor growth of orthotopic xenografts. We observed non-canonical activation of *GLI1* in claudin-low and EMT cell lines, and identified crosstalk with the NFκB pathway.

**Conclusions:** This work highlights the importance of *GLI1* in the maintenance of characteristics of metastatic breast cancer stem cells. Remarkably, treatment with an inhibitor of the NFκB pathway reproducibly reduces *GLI1* expression and protein levels. We further provide direct evidence for the binding of the NFκB subunit p65 to the *GLI1* promoter in both EMT and claudin-low cell lines. Our results uncover crosstalk between NFκB and *GLI1* signals and suggest that targeting these pathways may be effective against the claudin-low breast cancer subtype.

## Introduction

Breast cancer is a leading cause of cancer-related death in women. There are five major intrinsic breast cancer subtypes each with its own molecular characteristics, prognosis, incidence, and response to treatment [1]. Claudin-low tumors are mainly triple-negative invasive ductal carcinomas with a high frequency of metaplastic and medullary differentiation. There are conflicting reports as to the prevalence of these tumors, ranging from

as low as 1.5% of tumors [2] to 5 to 14% of breast tumors [3-5]. Claudin-low tumor cells are enriched for characteristics of tumor-initiating cells and across a differentiation spectrum are most similar to mammary epithelial stem cells [5]. Claudin-low breast cancers are characterized by low expression levels of cell-cell adhesion molecules including E-cadherin and several of the tight junction claudin proteins, claudin 3, 4, and 7. This subtype is molecularly similar to cells that have undergone an epithelial-to-mesenchymal transition (EMT) and overlaps with the recently characterized mesenchymal and mesenchymal stem-like subclassifications of triple-negative breast cancer [6,7]. Little is known about

\* Correspondence: scolavito@uwlax.edu

<sup>1</sup>Department of Pathology and Yale Cancer Center, Yale University School of Medicine, New Haven, CT 06520, USA

<sup>2</sup>Department of Biology, University of Wisconsin La Crosse, La Crosse, WI 54601, USA

molecular therapeutic targets in this highly aggressive subtype of breast cancer.

EMT cells undergo a morphological transition from the epithelial polarized phenotype to the mesenchymal fibroblastoid phenotype. This process is marked by loss of cell-cell adhesion molecules, such as E-cadherin, downregulation of epithelial differentiation markers, and upregulation of mesenchymal markers. In cancer, it is hypothesized that EMT cells gain migratory potential at the expense of proliferative ability. EMT has therefore been implicated in the process of metastasis. There is a close association between the EMT core signature and the signatures that define the claudin-low and metaplastic breast cancer subtypes [7].

In vertebrates, canonical Hedgehog (Hh) pathway signal transduction occurs when one of the three ligands, Sonic, Indian, or Desert hedgehog, binds to the receptor Patched-1 (*PTCH1*) or its homolog, Patched-2. In the off-state, *PTCH1* inhibits the activity of Smoothed (SMO). When stimulated by ligand this repression is lifted due to internalization and degradation of *PTCH1*. SMO then promotes the dissociation of the Suppressor of fused-Gli complex through an unknown mechanism. This allows for translocation of glioma-associated oncogene 1 (*GLI1*) and *GLI* family zinc finger 2 (*GLI2*) to the nucleus and degradation of the repressor form of *GLI* family zinc finger 3 (*GLI3*). In the nucleus, activated *GLI* proteins stimulate the transcription of Hh target genes, including *PTCH1* and *GLII*. *PTCH1* is a *Gli* target, providing a negative feedback mechanism whereby the pathway is regulated. *GLI1* is the key final output of the Hh pathway, and *GLII* transcription is the most reliable marker of pathway activation [8]. The Hh pathway plays a critical role in vertebrate development, and is responsible for controlling cell fate, patterning, survival, proliferation and differentiation. In the adult organism Hh is active in the maintenance of stem cells [9]. Deregulation of this pathway can result in cancer.

There is evidence of a role for the Hh pathway in breast cancer. Some tumors exhibit loss of chromosomal regions containing *PTCH1* or amplification of regions containing *GLII* [10], and Hh expression in the stroma is important [11]. Additionally, there is evidence for loss of *PTCH1* expression due to promoter methylation in human breast cancer, which correlated with decreased expression in samples from human ductal carcinomas *in situ* (DCIS) and in invasive ductal carcinomas [12]. Similarly, SMO has been found to be ectopically expressed in approximately 70% of DCIS samples, and 30% of invasive breast cancers [13]. Despite strong evidence for Hh pathway activation in breast cancer, overall few mutations in Hh pathway components have been identified [14]. *GLII* is amplified in glioblastoma and has been implicated in other cancers. *GLII* expression in mice

causes mammary tumors with a basal-like phenotype [15]. Additionally, mammary stem cells are regulated by *Gli* transcription factors [16], and *GLI1* has been associated with poorer outcome in ER $\alpha$ <sup>-</sup> tumors [17] and overall [18,19].

The nuclear factor kappa-light-chain-enhancer of activated B cells (NF $\kappa$ B) pathway plays a role in inflammation, cell survival, and transformation in response to stimuli including stress, cytokines, and microbial antigens. NF $\kappa$ B proteins are transcription factors, and inappropriate regulation of this family has been implicated in inflammatory and autoimmune diseases as well as cancer. Subunits of NF $\kappa$ B include v-rel avian reticuloendotheliosis viral oncogene homolog (Rel) family members RELA/p65, RELB, and c-REL, and NF $\kappa$ B subfamily members p105/p50 and p100/p52. NF $\kappa$ B family members associate with nuclear factor of kappa light polypeptide gene enhancer in B-cells inhibitor, alpha (I $\kappa$ B $\alpha$ ), which sequesters them in the cytoplasm, and they are generally not active unless they dimerize with Rel subfamily members. NF $\kappa$ B has been implicated in the progression of breast cancer. For example, NF $\kappa$ B promotes cell migration and metastasis by upregulating expression of chemokine receptor CXCR4 [20]. CXCR4 is highly expressed in metastases from breast cancer patients, and is thought to play a role in homing of tumor cells to the bone marrow.

In order to identify possible drivers of proliferation in mesenchymal stem-like breast cancer, we conducted an inhibitor screen of human mammary epithelial cells (HMLE) induced to undergo an EMT. The results indicate the importance of *GLI1* signaling in these cells, which further extended to a panel of claudin-low cancer cell lines. We identified non-canonical NF $\kappa$ B activation of *GLII* in these cells, indicating crosstalk between *GLI1* signaling and NF $\kappa$ B pathways in claudin-low and EMT breast cancer cells and suggesting a therapeutic route for claudin-low breast cancer.

## Methods

The experiments described did not include human subjects. All tumor data analyzed came from published expression datasets, which sought and obtained ethical approval and used Institutional Review Board approved protocols [5]. All animal studies were conducted in accordance with international, national, and university approved laws and policies. The animal studies received ethical approval from Yale University's Institutional Animal Care and Use Committee.

## Cell culture

HMLE-EMT and control cell lines were a gift of Robert A. Weinberg (Massachusetts Institute of Technology, Cambridge, MA) and were propagated as previously

described [21,22]. MTSV1-7 lines were a gift from Joyce Taylor-Papadimitriou [23]. Claudin-low cell lines, BT549, HS578T, MDA.MB.157, MDA.MB.231, and MDA.MB.436 as well as MCF10a, were obtained from American Type Culture Collection (ATCC) and propagated according to instructions. All experiments were done on low-passage cells.

#### High-throughput screen and dose-response curves

A total of 750 HMLE-shEcad cells per well were plated in 384-well plates in 20  $\mu$ l of growth media and allowed to adhere overnight. The following day 10 nl of compounds from stock plates were added to each well (Table S1 in Additional file 1). The stock plates contained each agent at 16 concentrations from 10 mM to 0.3 nM. Seventy-two hours after drug addition, viability was assayed using CellTiter-Glo reagent (Promega, Madison, WI, USA). The protocol for the screen has been previously described by our laboratory [24].

For generating dose-response curves manually, 1,000 cells/well in 100  $\mu$ l of media were plated in 96-well plates. Drug treatment and viability analysis was conducted as described above. Dose-response curves were generated using Graphpad Prism with Michaelis-Menten kinetics (Graphpad Software, Inc., San Diego, CA, USA).

#### RNA isolation and real-time PCR

RNA was isolated using the RNeasy Plus kit (Qiagen, Germantown, MD, USA) and cDNA synthesized using the iScript kit (Bio-Rad Laboratories, Hercules, CA, USA) according to manufacturers' protocols. Real-time PCR was performed on a Bio-Rad iCycler after combining the cDNAs with TaqMan universal PCR master mix and premixed FAM-labeled TaqMan probes (Applied Biosystems, Foster City, CA, USA). Abundance of mRNAs relative to *GAPDH* controls was calculated using the  $2^{-\Delta\Delta C_t}$  method.

#### Cell lysis and immunoblotting

Lysates were prepared from subconfluent cells using NP40 lysis buffer (1.0% NP40, 150 mM NaCl, 50 mM Tris-HCl pH 7.4, 5 mM EDTA, 10% glycerol) with phosphatase and protease inhibitors added. Lysates were transferred to polyvinylidene fluoride membranes and blocked in 5% nonfat milk in phosphate-buffered saline (PBS) with 0.1% Tween-20 (PBST). The primary antibodies used recognize GLI1, pEGFR, and ERBB2 (Cell Signaling Technology, Danvers, MA, USA) or epidermal growth factor receptor (EGFR), glyceraldehyde phosphate dehydrogenase (*GAPDH*) (Santa Cruz Technology, Santa Cruz, CA, USA). Membranes were washed with PBST and incubated with horseradish peroxidase-conjugated secondary antibodies. Gli1 blots were blocked in 5% bovine serum albumin (BSA).

#### Gene expression analysis of tumors

Analysis of published expression data (Gene Expression Omnibus: GSE18229) from 337 mammary tumors and primary tissue was conducted using the UNC337 dataset [5]. The expression level of *GLI1* across the predefined subtypes was determined for each dataset following median centering using GEO2R. Results were analyzed by one-way analysis of variance (ANOVA).

#### shRNA and retroviral infection

The following short hairpin (sh)RNA sense sequences were cloned into the pSIREN-RetroQ (BD Biosciences, Franklin Lakes, NJ, USA) shRNA-expressing retroviral vector: *GLI1* #1: CCCAGATGAATCACCAAATTCAA GAGATTT [25] and #2: AAGCGTGAGCCTGAATCTG TG [26]. *RELA*: GCTGTGTTTCACAGACCTGGCATCCG TCGA [27]. *NFKB1*: GCCAGAGTTTACATCTGA [28]. The negative control vector contains a scrambled sequence of a luciferase-directed shRNA (BD Biosciences).

For inducible shRNA-expressing viruses targeting *RELA*, the RHS4430-200223785 and RHS4430-200229897 GIPZ clones were purchased from Thermo Fisher Scientific (Waltham, MA, USA) and cloned in to pInducer10 via MluI and XhoI. Non-targeting sense sequence was 5'-GGATTCCAATTCAGCGGGAGCCTG-3' [29]. Virus was produced by co-transfection of the pInducer10 constructs and packaging plasmids into 293 T cells. Virus was harvested and concentrated, and cells were infected and selected as described above. To induce expression of the hairpin, cells were treated with 1  $\mu$ g/ml doxycycline for three days.

shRNA-expressing retroviruses were produced by co-transfection of the retroviral plasmids, pVSV-G and pCL-ECO (Clontech, Mountain View, CA, USA), into HEK 293 T cells (ATCC) using FuGene6 (Roche, Basel, Switzerland). Retrovirus was harvested in OptiMEM (Invitrogen) for five days, pooled, and concentrated with Centricon plus-20 columns (Millipore, Billerica, CA USA). Cells were infected at a multiplicity of infection of approximately five and selected in medium containing 0.6  $\mu$ g/ml puromycin for at least three days before use.

#### Proliferation assay

Cells infected with retrovirus were plated in 6-well dishes in medium containing 0.6  $\mu$ g/ml puromycin. Every 24 hours, one well was trypsinized and counted using a Countess tissue culture counter (Invitrogen, Carlsbad, CA, USA).

#### Migration assay

Retrovirally infected cells were selected for three days in medium containing 0.6  $\mu$ g/ml puromycin, and plated in an 8.0  $\mu$ m pore cell culture insert (BD Biosciences) in medium containing 1% fetal bovine serum (FBS), above

medium containing 10% FBS. After 12 h, cells were scraped from the inside of the insert, and the insert was stained using Diff-Quik (Siemens, Erlangen, Germany). Cells in at least five fields of view were counted for each insert.

#### Colony formation assay

Retrovirally infected cells were selected for three days in medium containing 0.6 µg/ml puromycin and plated at limiting dilutions in growth medium containing 0.6 µg/ml puromycin. Colonies were grown for 12 to 14 days, stained with Diff-Quik (Siemens), and counted under light microscopy.

#### Sphere formation assay

A total of 40,000 cells were plated on 60 mm ultra-low attachment plates (Corning, Inc., Corning, NY, USA) in 4 mL of mammosphere growth medium (mammary epithelial basal medium (Lonza Group Ltd, Basel, Switzerland) with B27 supplement (Invitrogen), EGF (20 ng/mL), bFGF (20 ng/mL), heparin (7 µg/ml), and penicillin/streptomycin with 0.5% methylcellulose, adapted from [30]). Medium was replaced every 48 hours for 12 days, and spheres were counted under light microscopy.

For secondary sphere formation, primary sphere cultures were filtered using a 70 µm nylon cell strainer, to retain spheres of larger than 70 µm in diameter. Spheres were trypsinized until they dissociated to single cells. Cells were counted, and 20,000 cells were plated on the ultra-low attachment plates, following the same conditions as listed above for primary sphere formation.

#### Flow cytometry

Cells were plated at  $5 \times 10^4$  cells/well in 6-well format and allowed to adhere overnight. The following day, cells were treated with 0.02 µM JK184 or 0.0002% DMSO vehicle control. After four days, floating cells were combined with adherent cells harvested by trypsinization and analyzed by flow cytometry using the BD Biosciences Pharmingen (San Diego, CA, USA) FITC Annexin V Apoptosis Detection Kit I. Samples were analyzed with the BD FACScaliburS flow cytometer with recording of 15,000 events per sample. Each line was treated independently and analyzed in three biological replicates. Gates were based on negative control signals, and plots generated using FlowJo 8.8.2 (Tree Star, Inc., San Carlos, CA, USA).

#### Orthotopic xenograft studies

MDA.MB.436 cells with sh*GLII* or control shRNA were trypsinized, washed twice in sterile  $1 \times$  PBS, and resuspended 1:1 in growth factor reduced matrigel (BD Biosciences). Cells were maintained on ice until

injection.  $2 \times 10^6$  control (NT) cells were injected into the right fourth mammary fat pad of five-week-old female NOD/SCID mice (NOD.CB17-Prkdcscid/J, The Jackson Laboratory, Bar Harbor, ME, USA). A contralateral injection was conducted, with  $2 \times 10^6$  sh*GLII* cells injected into the left fourth mammary fat pad of each mouse.

Tumor growth was monitored using digital calipers, and tumor volume was calculated using the formula:  $W^2 \times L \times 0.5$ , where L is the longer dimension and W the shorter. After seven weeks, animals were sacrificed and the tumors excised and weighed.

#### Immunofluorescence

Cells were plated on glass chamber slides. The next day cells were washed twice with PBS and fixed in 2% paraformaldehyde with 0.1% Triton-X-100 in PBS for 15' at room temperature (RT). Cells were washed twice in PBS, and quenched in 100 mM glycine in PBS for 5' at RT. The slides were washed in PBS and permeabilized in 0.1% Triton-X-100 in PBS for 15' at RT with humidification, followed by blocking in 5% BSA in PBST for 30' at 37°C with humidification. Primary antibodies against p50 and p65 (Cell Signaling Technology) were diluted 1:250 with PBST and incubated overnight at 4°C with humidity. Slides were washed thrice with PBST, and incubated with Alexa Fluor 594-conjugated secondary antibody (Invitrogen) diluted 1:1000 in PBST for 1 h at RT. Slides were washed thrice with PBST and PBS, and mounted with Prolong Gold (Invitrogen).

#### Chromatin immunoprecipitation (ChIP) assay

ChIP was performed according to published protocols with minor modifications [31]. Briefly, cells grown to 80% confluency were fixed in 1% formaldehyde for 10' at RT, followed by 0.125 M glycine quench. Plates were rinsed twice with PBS, and adherent cells were scraped in ice-cold PBS and collected by centrifugation. Cells were lysed on ice in buffer with protease inhibitors (5 mM PIPES pH 8, 85 mM KCl, 1% v/v igepal) using a dounce homogenizer. After centrifugation, the nuclei pellet was lysed on ice in buffer containing protease inhibitors (50 mM Tris-HCl pH 8, 10 mM EDTA, 1% w/v SDS). The chromatin was sonicated on ice for 15' with a 30''-on/30''-off cycle using a Biorupter UCD-200 (Diagenode Inc., Denville, NJ, USA) set to high. The chromatin was cleared by centrifugation, and for each ChIP from  $10^7$  cells was diluted to 1 mL with buffer containing protease inhibitors (50 mM Tris-HCl pH 7.4, 150 mM NaCl, 1% v/v igepal, 0.25% w/v deoxycholic acid, 1 mM EDTA, pH 8). Antibody was added (Histone H3, p65, and IgG from Cell Signaling Technology) and incubated at 4°C overnight on a rotating platform.

A total of 30 µl of magnetic protein G beads (Cell Signaling Technology) were added to each ChIP, and



incubated on a rotating platform for 2 h at 4°C. Beads were washed twice with dilution buffer, three times with 100 mM Tris-HCl pH 9, 500 mM LiCl, 1% v/v igeal, 1% w/v doxycholic acid, and once with 100 mM Tris-HCl pH 9, 500 mM LiCl, 150 mM NaCl, 1% v/v igeal, 1% w/v doxycholic acid. Antibody/chromatin complexes were eluted in 100 µl buffer (50 mM NaHCO<sub>3</sub>, 1% w/v SDS) for 1 h at RT. The samples were adjusted to 0.54 M NaCl, and incubated at 67°C overnight to reverse the crosslinks.

Samples were treated with RNaseA, and purified using a PCR cleanup kit (Qiagen). Real-time PCR was conducted using iQ SYBR Green Supermix (Bio-Rad Laboratories) on a CFX96 Real-Time System thermal cycler (Bio-Rad Laboratories) with 15 µl reactions, in triplicate. The following primer sets were used: *GLI1* site 1: 5'-GGG TAAGGGCTGTTGAGGTA-3', 5'-AAATGCTTGTCTC CCAGTGG-3'; 2: 5'-GAGCTAGGATGTGGGAGGTC-3', 5'-TGAGAAACGGAGAGGCAGAG-3'; 3: 5'-AGGGT CGGAATAAGTGTGGT-3', 5'-GTGTGTATGGGGAG GAGGAG-3'; 4: 5'-CTCTCCTCCCCATACACAC-3', 5'-CTCTCAGCACATCCGAAAG-3'; 5: 5'-ACGCCAT GTTCAACTCGATG-3', 5'-GAGATCTGCCAAATCCT CAAGG-3'; 6: 5'-GCCCAATCCTTCTGAGACT-3', 5'-CGGGCAGAGTCATGGGGA-3'; GAPDH: 5'-TACTAG CGGTTTTACGGCG-3', 5'-TCGAACAGGAGGAGCA GAGAGCGA-3'.

## Results

### EMT cells are more sensitive to GLI1 inhibitor

HMLE-shEcad cells are HMLE with E-cadherin knock-down [21], which results in EMT associated with mesenchymal-like and stem-like characteristics [7,22]. In order to identify possible drivers of proliferation, these cells were assayed for growth inhibition by a panel of 150 compounds at 16 doses each. Overall, the HMLE-shEcad cells were more resistant to this panel of inhibitors than were the control HMLE-shGFP cells (Figure 1A and Table S1 in Additional file 1). In every case where the response between the two cell lines differed by an IC<sub>50</sub> value of more than 0.01 µM for standard of care therapies for triple-negative breast cancer, the HMLE-shEcad cell lines had a poorer response (higher IC<sub>50</sub> value) than the control cell line.

Interestingly, epidermal growth factor receptor (EGFR) inhibitors erlotinib and gefitinib profoundly inhibited the proliferation of the control cell lines, while the EMT cell lines were resistant to this treatment, with neither EGFR inhibitor approaching 50% growth inhibition at concentrations up to 10 µM (Figure S1A-C in Additional file 1). In follow-up studies we observed that despite having an intact EGFR pathway, HMLE-shEcad cells lack high levels of baseline phosphorylated EGFR, and have lower levels of EGFR overall, possibly rendering them

immune to EGFR-inhibitor treatment, and suggesting that the cells do not rely on EGFR signaling for survival. ERBB2 levels do not differ between control or EMT cells (Figure S1D-F in Additional file 1). The lack of response to EGFR inhibition is in concordance with the recent finding that activation of the EMT program effects a shift from EGFR to platelet-derived growth factor receptor (PDGFR) signaling [32].

While the HMLE-shEcad cells were more resistant overall to the panel of inhibitors, there were a few compounds that selectively inhibited the growth of the EMT cells compared to controls. One such agent was the GLI1 inhibitor JK184 [33], which was more active against HMLE-shEcad cells than controls. The IC<sub>50</sub> value for JK184 was 3.5-fold lower for the HMLE-shEcad cells compared to the control HMLE-shGFP cell line (0.004 µM compared to 0.014 µM, Figure 1B). The dose-response curve for the HMLE-shEcad cells was shifted to lower doses compared to the HMLE-shGFP curve, indicating a concentration window between 0.001 to 0.1 µM in which JK184 is more effective on the EMT cells. This selective sensitivity to the GLI1 inhibitor was confirmed in another EMT cell line, HMLE-Snail [22], which was similarly more sensitive to JK184 compared to HMLE-pBP control cells (Figure 1C). Immunoblot and real-time PCR analysis indicated that both EMT cell lines have higher protein and transcript levels of *GLI1* than controls, as well as elevated levels of *GLI2*, while the extent of *GLI3* expression was consistent across the cell lines (Figures 1D and 2B).

Treatment of both EMT cell lines with the IC<sub>25</sub> and IC<sub>50</sub> doses of JK184 yielded a dose-dependent decrease in *GLI1* protein and transcript levels (Figure 1D-E). GLI1 positively regulates its own transcription [34], so it is likely that the JK184-dependent decrease in *GLI1* transcript and protein levels arises from decreased activity of the JK184 target GLI1. *GLI2* and *GLI3* are not direct targets of GLI1, and neither *GLI2* nor *GLI3* transcript levels were affected in JK184-treated HMLE cells (Figure S2A-B in Additional file 1).

### Claudin-low cell lines express elevated levels of Gli proteins and are more sensitive to the GLI1 inhibitor

We next determined if Gli expression is associated with a particular breast cancer subtype. Using a previously published dataset, cell lines were clustered based on CD24, CD44, E-cadherin (CDH1), and CLDN3, 4, and 7 expression status [35]. This reveals a subgroup of basal B cell lines identified as claudin-low [5,36]. Claudin-low tumors express decreased levels of *CDH1*, are enriched for EMT markers, and are CD24 low/CD44 high, which are features of self-renewing breast cancer stem cells [5].

Within the basal subtype, the claudin-low cells generally express higher levels of *GLI1*, *GLI2*, and *GLI3*

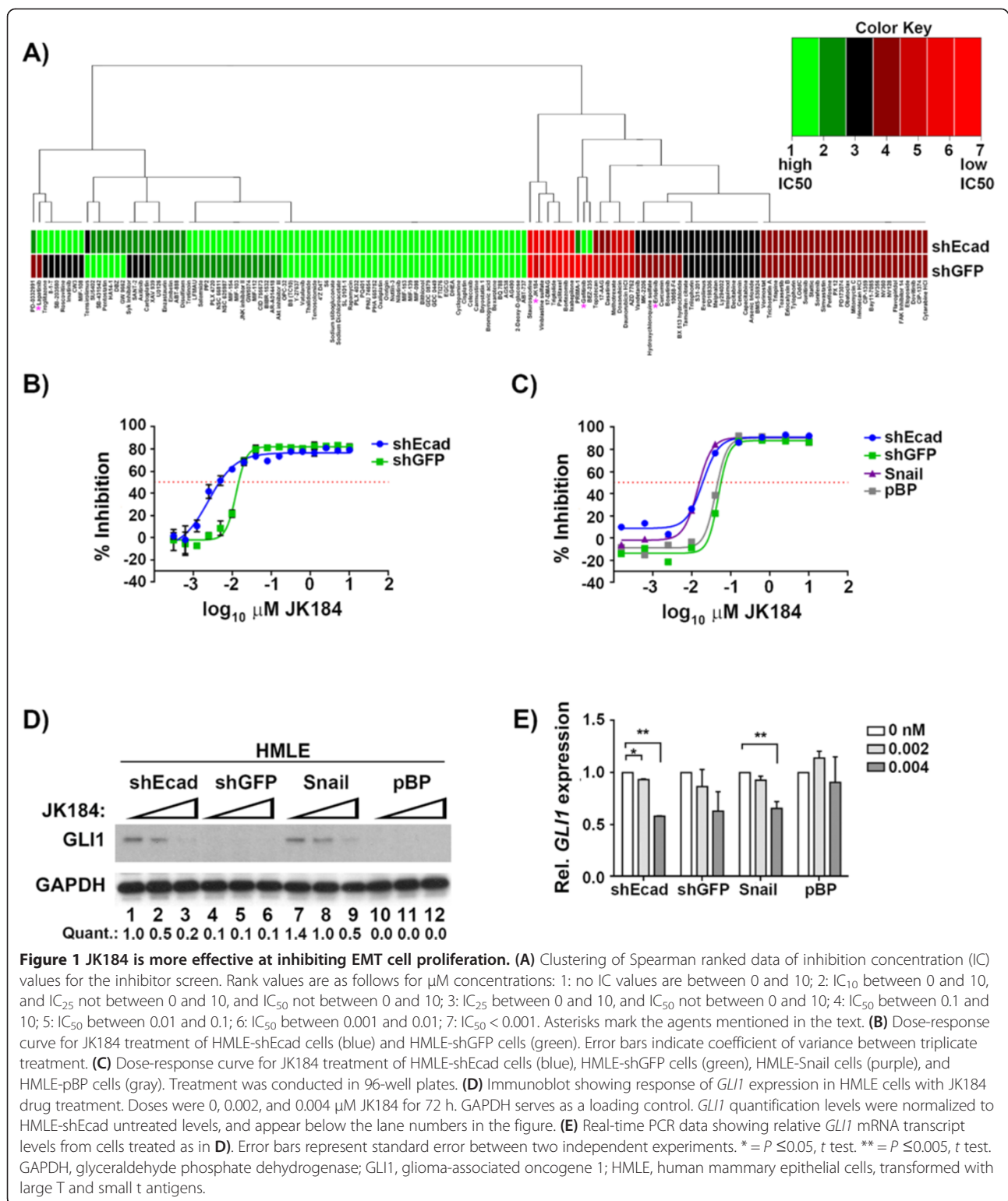


(Figure 2A). We confirmed this expression data in several claudin-low cell lines, and found that similarly to the EMT cell lines, claudin-low cells express higher transcript levels of the Gli family of transcription factors than

do MCF10a cells, an immortalized but non-tumorigenic mammary cell line (Figure 2B). Additionally, claudin-low cell lines have higher protein levels of *GLI1* than do MCF10a cells (Figure 2C).

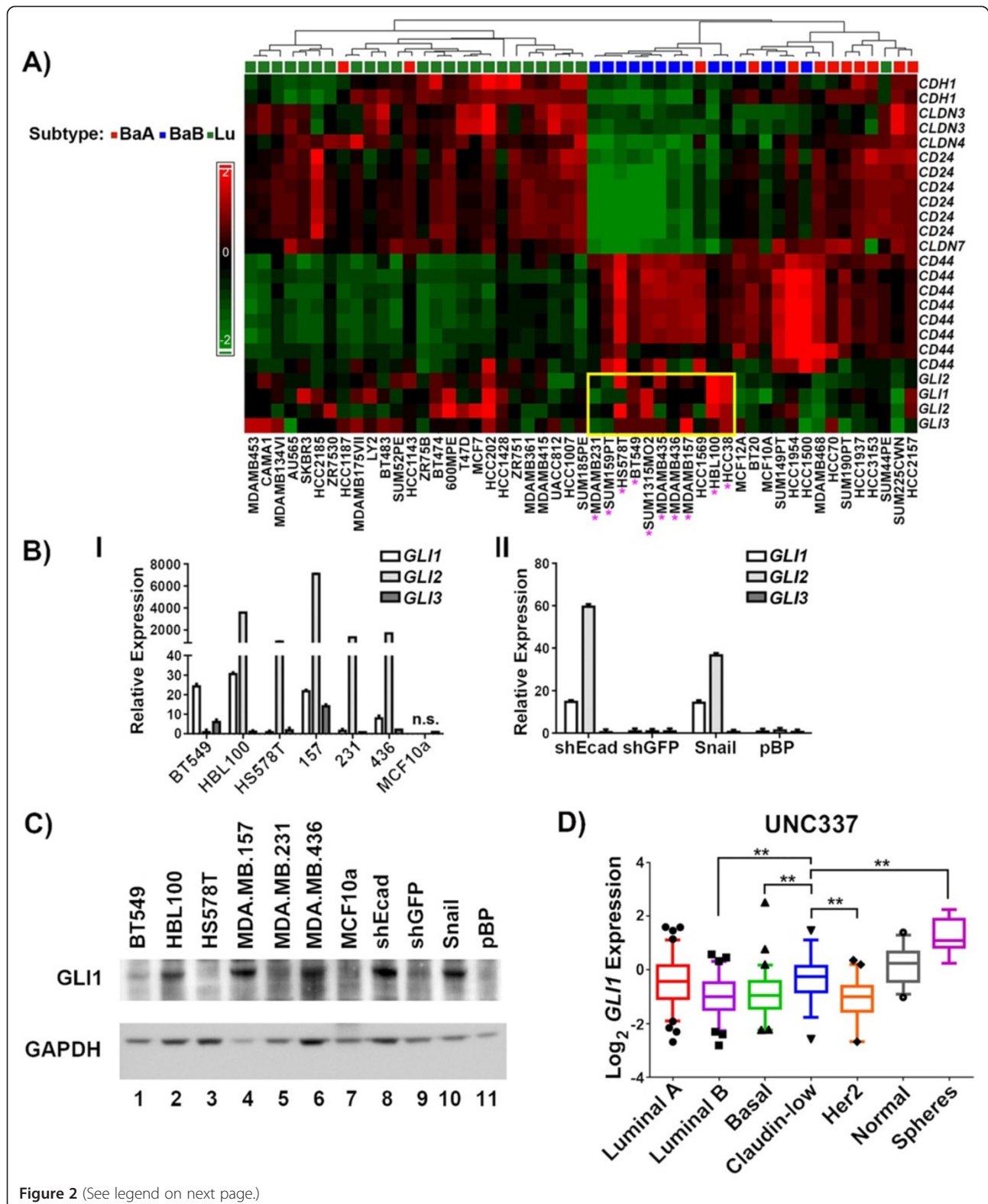


Figure 2 (See legend on next page.)

(See figure on previous page.)

**Figure 2 Claudin-low cell lines express higher transcript and protein levels of *GLI1*.** (A) Expression of *CD44*, *CD24*, *CDH1*, *Gli*, and *CLDN3*, 4, and 7, transcripts across a panel of breast cancer cell lines [34]. Multiple probes for each gene were extracted from microarray data and their expression values were Z transformed and plotted as a heat map. BaA = basal A, BaB = basal B, Lu = luminal. Asterisks denote cell lines originally identified as claudin-low [5]. Yellow box surrounds the expression of Gli family members in claudin-low cell lines. (B) Graph of relative Gli family expression levels in claudin-low (I) and EMT (II) cell lines, relative to controls. Error bars represent standard error, and n.s. indicates that no signal was achieved under the parameters used. (C) Immunoblot of *GLI1* levels in the indicated claudin-low cell lines. *GAPDH* serves as a loading control. (D) Plot of *GLI1* expression data from UNC337 mammary tumor and tissue dataset, based on subtype. 99% confidence interval is shown, with outliers plotted as single data points. Significance was calculated using one-way ANOVA using multiple comparisons, and all significant comparisons between the claudin low data set and others are indicated. \*\* =  $P \leq 0.005$ . ANOVA, analysis of variance; EMT, epithelial-to-mesenchymal transition; *GAPDH*, glyceraldehyde phosphate dehydrogenase; *GLI1*, glioma-associated oncogene 1.

Given the elevated expression levels of *GLI1* we observed in claudin-low cell lines, we determined if claudin-low tumors display similarly elevated *GLI1* levels. An analysis of a published dataset of over 330 tumors, including 37 claudin-low tumors, revealed elevated *GLI1* expression levels in claudin-low tumors compared to basal tumors ( $P = 0.001$ , Figure 2D). Some luminal A tumors express *GLI1*, which mirrors the expression data for the cell lines (Figure 2A).

Since claudin-low cell lines and tumors preferentially express *GLI1* transcripts, and claudin-low cells are transcriptionally similar to the JK184-sensitive EMT cells, we determined the dose-sensitivity of claudin-low cell lines to JK184. Overall, claudin-low cell lines are more sensitive to JK184 treatment than are MCF10a, MTSV1-7, or HMLE-shGFP and HMLE-pBP cells, and JK184 induced a dose-dependent decrease in *GLI1* transcript and protein levels in these cells (Figure 3A-C). *GLI2* and *GLI3* levels were not significantly altered with JK184 treatment (Figure S2C-D in Additional file 1). Taken together, these data establish similar patterns of *GLI1* signaling and *GLI1* inhibitor sensitivity in EMT and claudin-low cell lines, providing further evidence for the similarity of EMT and claudin-low cells.

#### **GLI1 inhibitor treatment results in increased apoptosis**

Since JK184 treatment reduced cell accumulation, we identified whether there is an elevated rate of apoptosis in JK184-treated cells. Treatment with the  $IC_{50}$  dose of JK184 enhanced the proportion of HMLE-shEcad cells that stained with Annexin-V, but were negative for propidium iodide (PI) ( $P < 0.0001$ ,  $t$  test; Figure 3D). This staining pattern is consistent with early-apoptotic cells, while PI-positive or dual-stained cells indicate apoptosis and/or necrosis. JK184-treated cells were sparser and less well spread than vehicle-treated counterparts (Figure 3D). JK184 treatment did not significantly affect the staining of HMLE-shGFP cells or their morphology (Figure 3D). Over four days of treatment there was increased cell death of the BT549 cells, as increased Annexin-V and PI staining were observed in

treated cells, and these cells appeared rounded up compared to vehicle-treated counterparts ( $P = 0.001$ ,  $t$  test; Figure 3D).

#### **Knockdown of *GLI1* decreases proliferation of claudin-low cell lines**

Given the markedly elevated *GLI1* levels observed in the claudin-low subtype, we wanted to determine the biological importance of *GLI1* in claudin-low cell lines. We investigated the effects of *GLI1* knockdown on aggressive characteristics of claudin-low tumor cells, including proliferation, migration, and anoikis. *GLI1* has been implicated in several of these processes in transformed cells [37] and in some breast cancer cell lines [38]. Since there did not always appear to be a direct correlation between expression levels of *GLI1* and sensitivity to JK184 treatment, and to avoid possible off-target effects of JK184, we utilized a specific genetic approach to reduce *GLI1* expression. Two different shRNA viruses both induced stable, specific knockdown of *GLI1* protein (Figure 4A) and transcript levels (Figure 4B). Neither *GLI2* nor *GLI3* transcript levels were affected by *GLI1* knockdown (Figure S2E-F in Additional file 1). Knockdown of *GLI1* in MDA.MB.157 cells resulted in cells that appeared rounder and less elongated compared to cells with control knockdown, which maintained the long spindle shape characteristic of mesenchymal cells (Figure 4C). MDA.MB.157 cells have an extended doubling time of greater than 60 hours, so we therefore evaluated the biological effects of *GLI1* knockdown in two other claudin-low cell lines with high *GLI1* expression, BT549 and MDA.MB.436 cells. Knockdown of *GLI1* greatly reduced the growth rates of these cell lines compared to cells expressing the non-targeting shRNA (Figure 4D-E). Proliferation of MCF10a cells, which do not express endogenous *GLI1*, was not significantly affected by infection with the sh*GLI1* retrovirus (Figure S3F in Additional file 1). The proliferation of the immortalized human mammary epithelial cell line MTSV1-7 was significantly, though slightly, impaired following *GLI1* knockdown. These cells do express some *GLI1* (Figure S3A-C, F in Additional file 1).



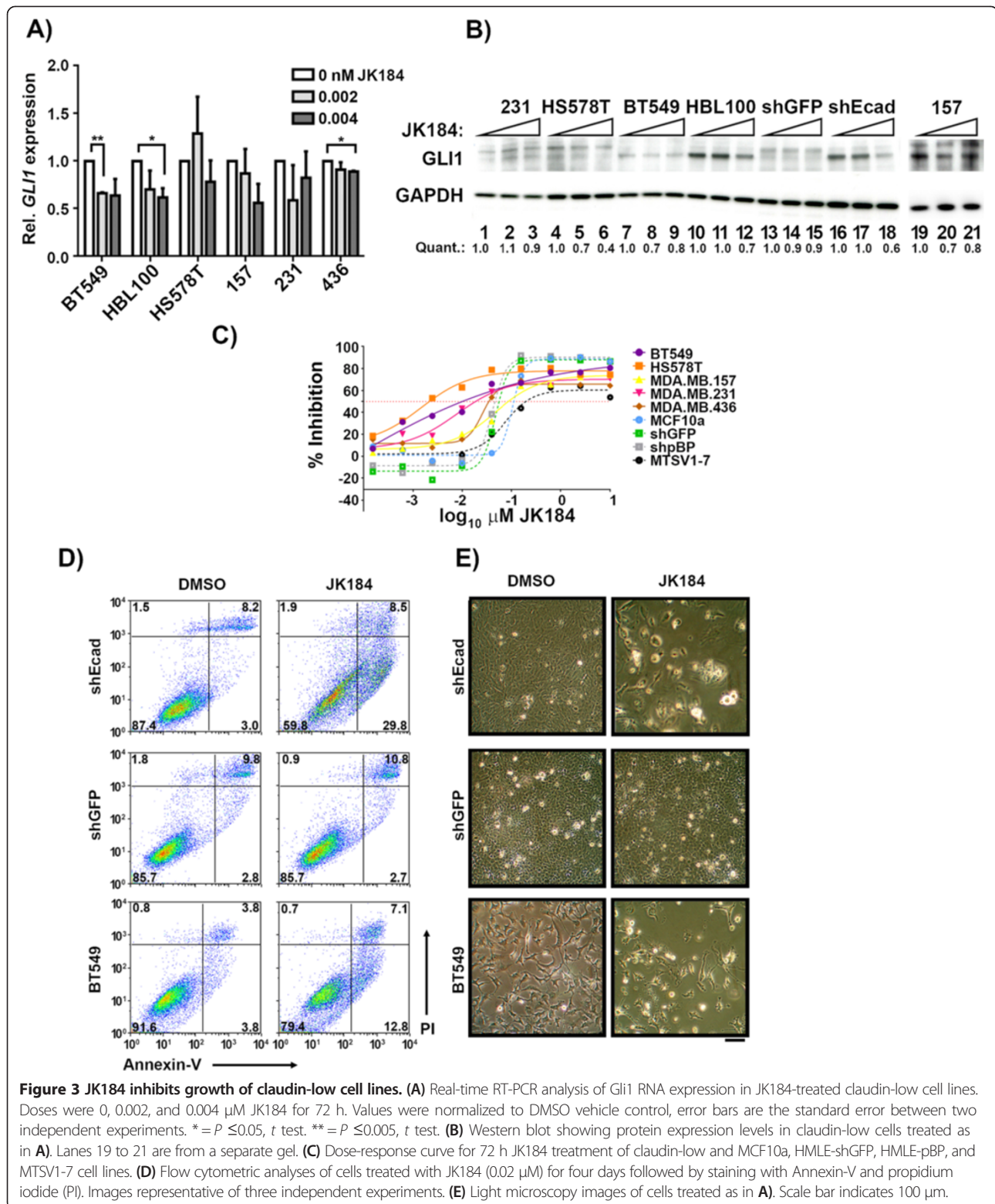
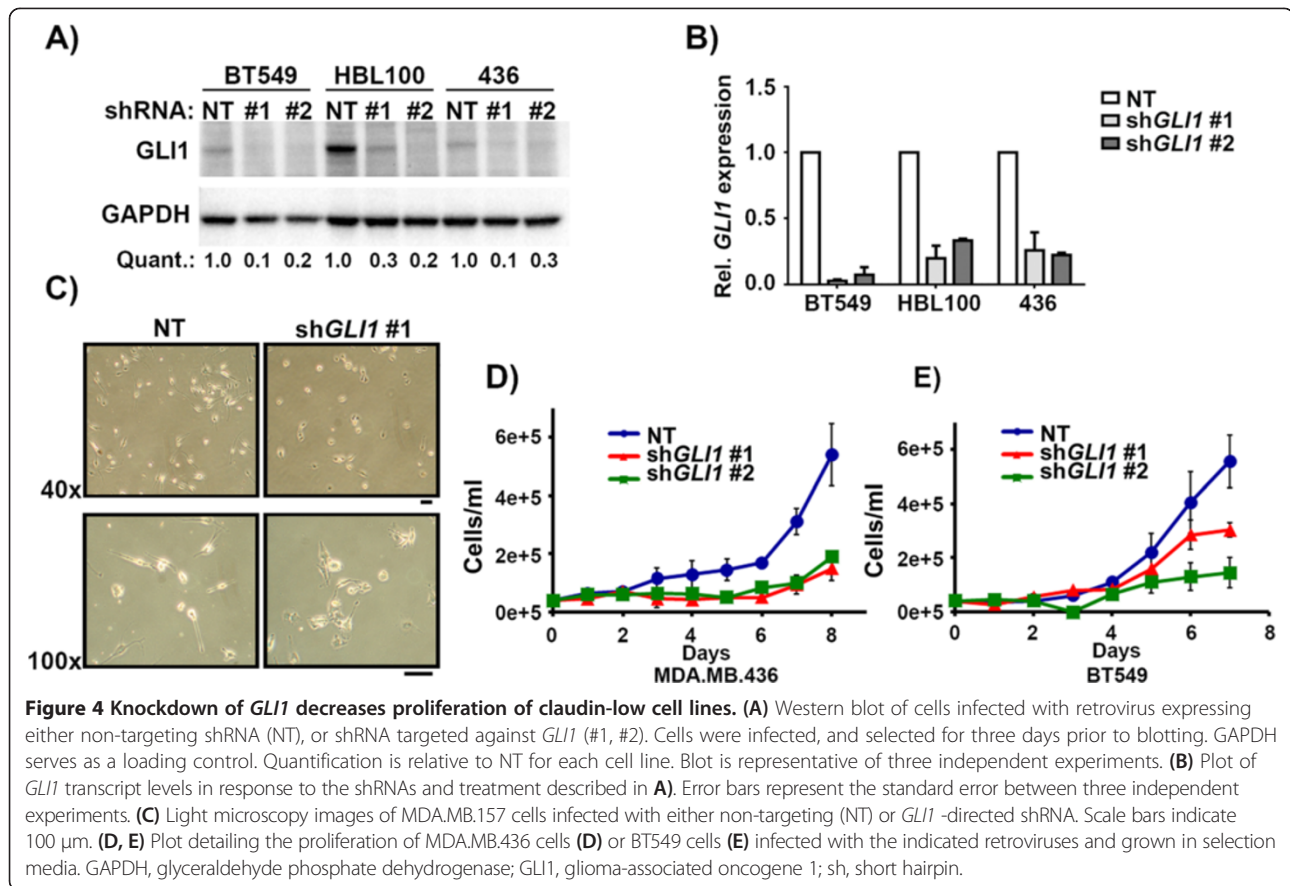


**Figure 3 JK184 inhibits growth of claudin-low cell lines.** (A) Real-time RT-PCR analysis of *GLI1* RNA expression in JK184-treated claudin-low cell lines. Doses were 0, 0.002, and 0.004 μM JK184 for 72 h. Values were normalized to DMSO vehicle control, error bars are the standard error between two independent experiments. \* =  $P \leq 0.05$ ,  $t$  test. \*\* =  $P \leq 0.005$ ,  $t$  test. (B) Western blot showing protein expression levels in claudin-low cells treated as in (A). Lanes 19 to 21 are from a separate gel. (C) Dose-response curve for 72 h JK184 treatment of claudin-low and MCF10a, HMLE-shGFP, HMLE-pBP, and MTSV1-7 cell lines. (D) Flow cytometric analyses of cells treated with JK184 (0.02 μM) for four days followed by staining with Annexin-V and propidium iodide (PI). Images representative of three independent experiments. (E) Light microscopy images of cells treated as in (A). Scale bar indicates 100 μm.

### Loss of *GLI1* reduces cell migration and anchorage-independent growth

*GLI1* knockdown significantly reduced the transwell migration of BT549 and MDA.MB.436 cells in response to

an FBS gradient with both *GLI1* knockdown constructs used (Figure 5A). The low FBS in the top chamber of the transwell (1%) and the relatively short assay time (12 h) minimized the impact of reduced proliferation

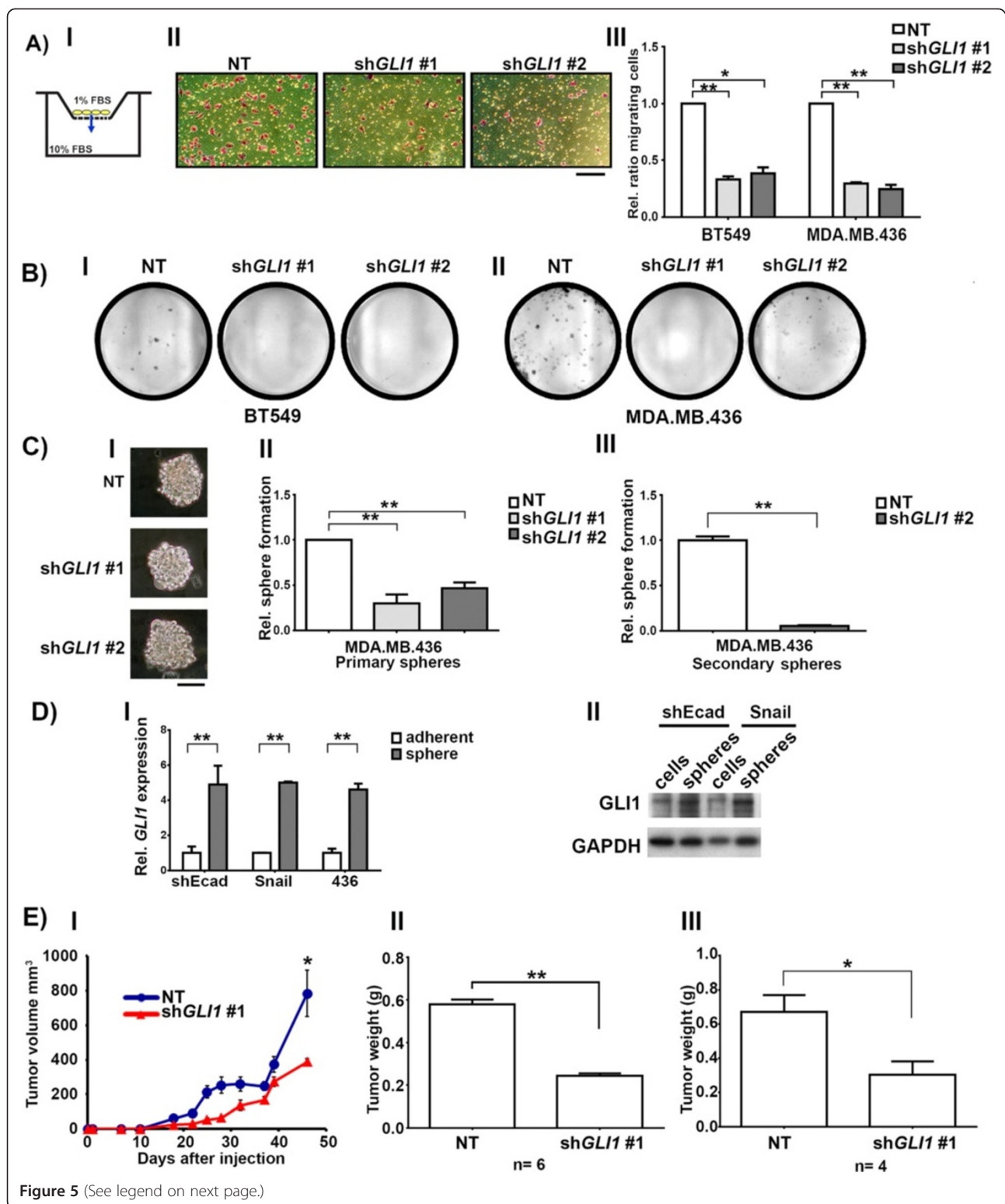


resulting from *GLI1* knockdown. MCF10a cells were not affected (Figure S3E in Additional file 1).

In clonogenicity assays, knockdown of *GLI1* reduced colony formation of BT549 and MDA.MB.436 cells (Figure 5B), whereas MCF10a cells were largely unaffected (Figure S3D in Additional file 1). Mammospheres are derived from mammary cells grown under non-adherent conditions. They are enriched in early progenitor/stem cells and are able to differentiate along all three mammary epithelial lineages [30]. The sphere-initiating subset of mammary cells have cancer stem cell-like characteristics, including the ability to self-renew and to differentiate into mature mammary cells that lack stem cell features [16,30]. We did not observe any significant sphere formation resulting from either the control HMLE-shGFP or HMLE-pBP cell lines, as has been previously reported [22]. We also did not achieve significant levels of spheres resulting from BT549 cells, despite their tumorigenicity [39]. Therefore, we first investigated the effects of *GLI1* knockdown on the sphere-forming ability of MDA.MB.436 cells. *GLI1* knockdown reduced primary and secondary sphere formation by MDA.MB.436 cells (Figure 5C). Secondary sphere formation is a measure of the self-renewal capacity of the

sphere-forming cells. The ability of the cells to form secondary spheres was enhanced compared to primary sphere forming ability, producing on average 454 secondary spheres from 20,000 plated cells (0.055%), compared to the average primary sphere forming ability of 254 spheres from 40,000 plated cells (0.006%). These data, combined with the higher *GLI1* transcript and protein levels we observed in spheres derived from EMT and/or claudin-low cells compared to control adherent cells (Figure 5D) indicates that *GLI1* is important for formation of spheres. Elevated *GLI1* levels were seen in primary mammospheres formed from normal and tumorigenic breast tissue from a published dataset (Figure 2D). Higher levels of *GLI1* transcripts in mammospheres compared to differentiated mammary cells has been reported [16,40], but we observed that *GLI1* levels in mammospheres are even higher than those in EMT cells grown under adherent conditions.

We also wanted to investigate the effects of *GLI1* knockdown in a basal cell line, HCC1806, which expresses elevated levels of *GLI1* (Figure S3A-C in Additional file 1). Significantly fewer spheres resulted from cells in which *GLI1* expression was reduced compared to controls (Figure S3G in Additional file 1). Additionally,



(See figure on previous page.)

**Figure 5 Decrease in *GLI1* expression inhibits cell migration and anchorage-independent growth.** (A) Panel I: Cartoon depicting experimental setup. Cells (yellow) were plated in the top of a Boyden chamber in 1% FBS above a lower-chamber of media containing 10% FBS. After 16 hours the number of cells that have migrated to the bottom side of the filter were stained and counted. II: Light microscopy images of the bottom side of the migration filter after staining. BT549 cells were infected with the indicated retroviruses and selected prior to experimentation. Scale bar indicates 100  $\mu$ m. III: Migration of BT549 and MDA.MB.436 cells infected with the indicated retroviruses and assayed as described in I. (B) Clonogenic colony formation assay in BT549 (I) and MDA.MB.436 (II) cells. (C) Panel I: Representative 12 day spheres formed in MDA.MB.436 cells infected with the indicated retroviruses. Scale bar indicates 100  $\mu$ m. II: Relative sphere formation by MDA.MB.436 cells. (D) Panel I: *GLI1* mRNA expression obtained from real-time RT-PCR analysis of mRNA from adherent cells incubated in mammosphere medium (white bars) or sphere cells grown under non-adherent conditions (gray bars). II: Western blot detailing *GLI1* levels in HMLE-shEcad or HMLE-Snail adherent and sphere cells. For all: \* =  $P \leq 0.05$ ,  $t$  test. \*\* =  $P \leq 0.005$ ,  $t$  test. (E) (I) Plot of tumor volume over time arising from orthotopic injection of MDA.MB.436 cells infected with either non-targeting (NT) or *GLI1* knockdown constructs.  $n =$  six animals. (II) Final averaged tumor weights at seven weeks post-injection for  $n =$  six animals. (III) Final averaged tumor weights from an independent biological replicate of the orthotopic xenograft study, conducted on four animals. FBS, fetal bovine serum; *GLI1*, glioma-associated oncogene 1.

similarly as to seen with the MDA.MB.436 cells and the EMT cell lines, there was significantly more *GLI1* expression from HCC1806 cells grown as spheres compared to those grown under adherent conditions (Figure S3H in Additional file 1). This is further evidence that *GLI1* is activated and functionally important in sphere-initiating and/or early progenitor cells across a spectrum of cell lines.

#### ***GLI1* expression is important for tumor formation *in vivo***

Having shown that *GLI1* is essential for the aggressive and stem-like characteristics of claudin-low cell lines *in vitro*, so we next examined the effects of *GLI1* knockdown *in vivo*. While previous studies have highlighted the ability of ectopic *GLI1* expression to form tumors *in vivo* [15,40], we wanted to investigate the effects of *GLI1* knockdown on the tumor-forming abilities of claudin-low MDA.MB.436 cells as orthotopic xenografts. While all sh*GLI1* expressing cells eventually formed tumors, *GLI1* knockdown tumors were smaller on average than tumors resulting from contralateral control knockdowns (Figure 5E, panel I and II). Similar results were seen for an independent biological replicate (Figure 5E, panel III, and Figure S4 in Additional file 1). These data are consistent with reports from other groups, in which knockdown of *GLI1* delayed onset of tumor formation from injection of claudin-low SUM1315 cells [40], and reduced the incidence of metastasis to the lung by claudin-low MDA.MB.231 cells [41].

#### **The NF $\kappa$ B pathway contributes to elevated *GLI1* levels in claudin-low and EMT cells**

Whereas JK184 reduced *GLI1* levels, cyclopamine, which inhibits the Hh pathway through SMO, did not affect proliferation or *GLI1* levels in EMT cells (Figure 6A-C). Additionally, two other SMO inhibitors in our screen had no effect on accumulation of EMT cells (Figure 6A). The ineffectiveness of cyclopamine on *GLI1* expression is consistent with published results for breast cancer cell lines including SUM149, T47D, MCF7, and MDA.

MB.231 [38,40,42]. Taken together, these data indicate that the elevated *GLI1* levels in EMT and claudin-low cell lines are not caused by classical activation of the pathway through SHH-PTCH1-SMO. Non-canonical activation of the Hh pathway can occur with activation of the Gli family, mainly *GLI1*, by MAPK/ERK [43], AKT [44], KRAS [45], mTOR/S6K1 [46], and more recently NRP2 [40]. The mechanisms of SMO-independent up-regulation of *GLI1* are poorly understood.

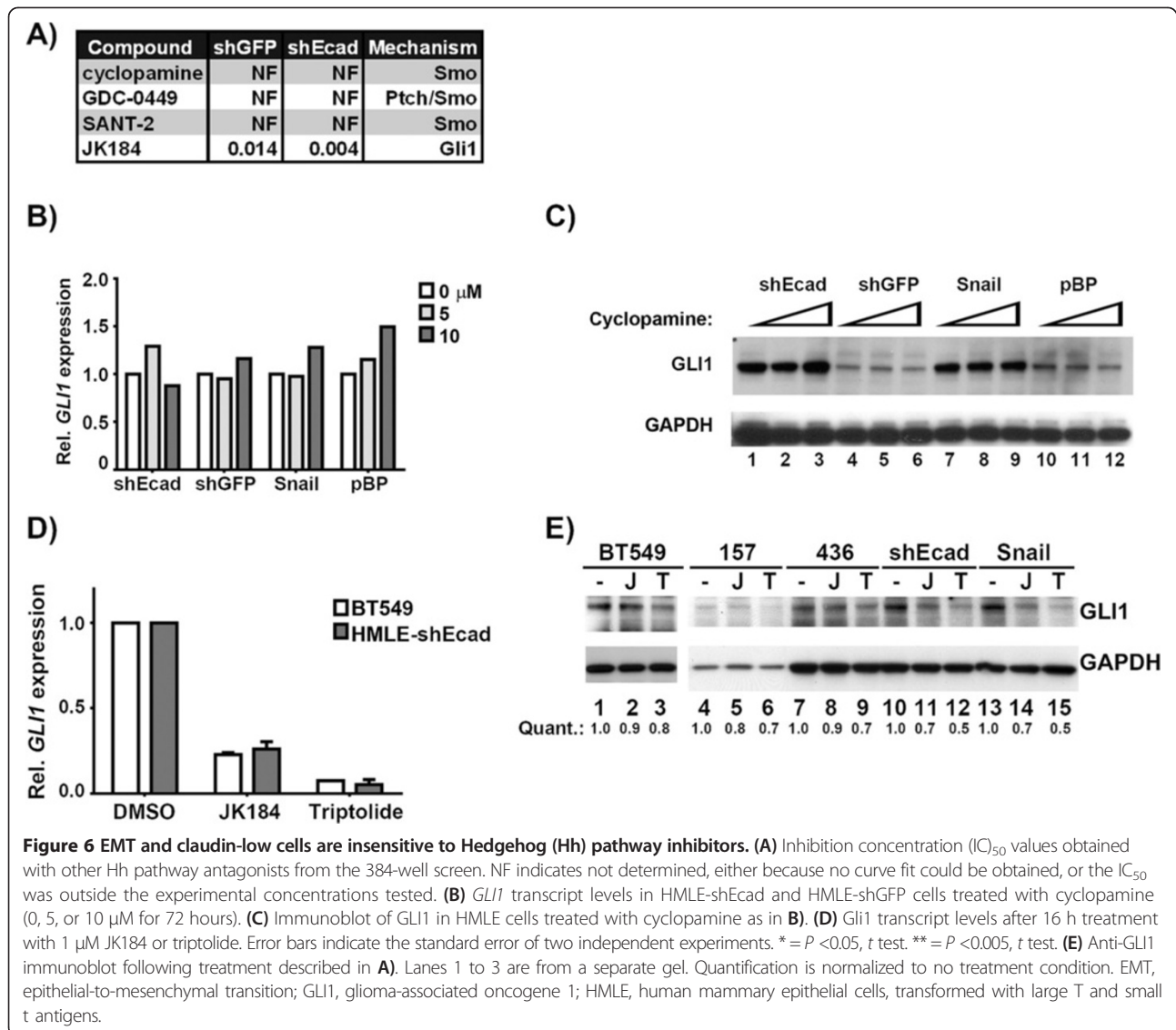
To determine which upstream pathways are responsible for elevated *GLI1* in claudin-low and EMT cells, we screened several candidate molecules for reduction of *GLI1* expression (Figure S5A-B in Additional file 1). Triptolide, an NF $\kappa$ B inhibitor [47-49] reduced *GLI1* transcript and protein levels in both HMLE-shEcad and BT549 cell lines (Figure 6D-E). The activity of triptolide as an NF $\kappa$ B inhibitor was confirmed by means of a reporter assay (Figure S5C in Additional file 1).

Since we observed these effects without stimulation or activation of the NF $\kappa$ B pathway, we hypothesized that NF $\kappa$ B is basally activated in our cells. Normally, NF $\kappa$ B subunits are sequestered in the cytoplasm due to inhibitory interactions with I $\kappa$ B. However, we observed that both the p65 and p50 subunits of NF $\kappa$ B present in the nucleus of EMT cells, while they are restricted to the cytoplasm of the HMLE control cell lines (Figure 7A). p65 and p50 show a similar localization pattern for claudin-low versus MCF10a cells (Figure S6 in Additional file 1). These data suggest that NF $\kappa$ B is basally present in the nucleus of EMT and claudin-low cells, and active even without stimulation by a proinflammatory agent, in agreement with some earlier reports describing constitutive NF $\kappa$ B activity in basal cell lines [50-52].

#### **NF $\kappa$ B binds to the *GLI1* promoter in EMT and claudin-low cells**

The effects of triptolide on the expression levels of *GLI1* suggest that NF $\kappa$ B could act as a transcription factor to regulate *GLI1* expression. We searched the genomic region surrounding the transcription start site of





*GLI1* for potential  $\kappa$ B binding sites using SABiosciences DECipherment of DNA Elements (DECODE) system which searches for predicted binding sites of transcription factors using data from the ENCODE project consortium and the UCSC Genome Browser. Six potential  $\kappa$ B binding sites were identified that matched the consensus  $\kappa$ B binding sequence (Figure 7B). In order to determine if NF $\kappa$ B binds to the *GLI1* promoter we conducted ChIP experiments using primer sets designed to amplify each predicted binding site. Binding of the p65 subunit of NF $\kappa$ B to the first predicted  $\kappa$ B binding site (chr12: 57851125–57851134) was enriched over the other binding sites in unstimulated HMLE-shEcad cells (Figure 7C). The binding of histone H3 to the six potential  $\kappa$ B binding sites as well as to GAPDH serves as a positive control for the ChIP experiment (Figure 7C).

We also observed enrichment of p65 subunit binding to Site 1 in HMLE-Snail, BT549, and MDA.MB.436 cells (Figure S6B in Additional file 1). We did not detect enhanced binding of p65 subunits to Site 1 in the *GLI1* promoter of HMLE-shGFP or HMLE-pBP cell lines, despite observing enriched binding of histone H3 with Site 1, which serves as a positive control for the ChIP experiment (Figure S7A in Additional file 1). Overall the ChIP data suggest that there is crosstalk between NF $\kappa$ B and GLI1 signaling in EMT and claudin-low cell lines.

Since the NF $\kappa$ B inhibitor triptolide decreased the expression level of *GLI1*, we determined the impact of triptolide treatment on binding of p65 to the *GLI1* promoter. 1  $\mu$ M triptolide treatment for six hours caused a 70% reduction in binding of p65 to Site 1 in the *GLI1* promoter of HMLE-shEcad cells compared to control vehicle treatment (Figure 7D). This supports the conclusion that

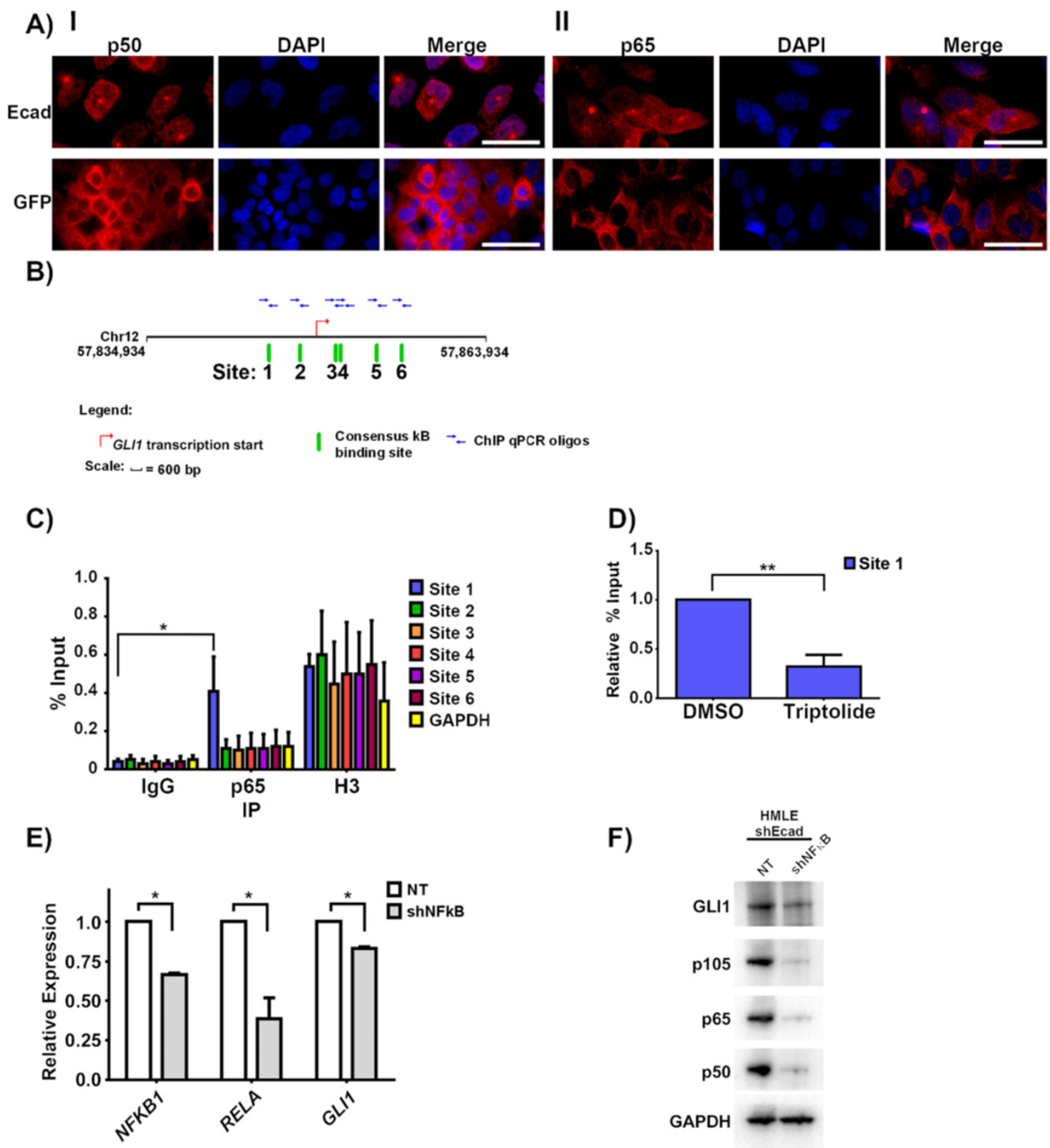


**Figure 7 Crosstalk between NFκB and GLI1 signaling pathways.** (A) Immunofluorescence images showing localization of NFκB p50 (Panel I) or p65 (Panel II) subunits in HMLE-shEcad (top row) or HMLE-shGFP (lower row) cells. Scale bar indicates 50 μm. (B) Map of putative NFκB binding sites surrounding the *GLI1* promoter. Red arrow marks transcription start site. Green lines indicate sequences matching the consensus kB binding site; putative sites are numbered 1 to 6. Blue arrows indicate primer sets used for ChIP. (C) ChIP of HMLE-shEcad cells with indicated antibodies. Error bars indicate standard error among three independent experiments. (D) NFκB p65 ChIP to the *GLI1* promoter (site 1) following six-hour treatment with 1 μM triptolide. Graph was normalized to binding with vehicle control (DMSO). Error bar indicates standard error among three independent experiments. (E) Real-time PCR data showing *RELA*, *NFKB1*, and *GLI1* transcript levels after infection of HMLE-shEcad cells with non-targeting (NT) or shRELA and shNFKB1 virus (shNFKB) virus. (F) Western blot of Gli1, p65, and p50 levels in HMLE-shEcad cells infected with either non-targeting (NT) or shRELA and shNFKB1 virus (shNFKB). GAPDH serves as a loading control. For all: \* =  $P \leq 0.05$ , *t* test. \*\* =  $P \leq 0.005$ , *t* test. ChIP, chromatin immunoprecipitation; GLI1, glioma-associated oncogene 1; RELA, v-rel reticuloendotheliosis viral oncogene homolog A; NFKB1, nuclear factor of kappa light polypeptide gene enhancer in B-cells 1; NFκB, nuclear factor kappa-light-chain-enhancer of activated B cells; sh, short hairpin.

triptolide decreases *GLI1* expression by inhibiting binding of NFκB transcriptional complexes to the *GLI1* promoter.

#### Knockdown of NFκB results in decreased *GLI1* expression

Although triptolide has been shown to inhibit NFκB, it is not entirely specific. In order to reinforce the connection between NFκB and elevated *GLI1* levels, we determined the impact of NFκB knockdown on *GLI1* expression. Combined reduction of *RELA* of approximately 60%, and of *NFKB1* by 40% reduced *GLI1* expression at both the protein and transcript level in HMLE-shEcad cells (Figure 7E-F) and similar results were seen with knockdown of both NFκB subunits in MDA.MB.436 cells (Figure S7C in Additional file 1). Doxycycline-inducible knockdown of *RELA* of approximately 75% with two separate hairpins reduced *GLI1* expression (Figure S7D in Additional file 1). Hence, *GLI1* is regulated by NFκB in claudin-low and EMT cells.

#### Discussion

Currently, there are no targeted treatment options for patients with claudin-low breast cancer, a particularly aggressive type of breast cancer. We used mammary carcinoma cell lines with induced EMT as surrogates for cells with stem-like characteristics and screened them for growth sensitivity to 150 targeted agents. Selective sensitivity of these cells to inhibition of *GLI1* implicated *GLI1* as a vulnerable target. The transcriptional similarities of induced EMT mammary cells to claudin-low breast cancer suggested the potential importance of *GLI1* for this breast cancer subset. Reduced *GLI1* expression impeded migration, clonogenicity, primary and secondary mammosphere formation and tumor formation by claudin-low breast cancer cells. These characteristics are associated with stem-like, invasive, and aggressive aspects of breast cancer, and suggest that inhibiting *GLI1* may be an effective treatment strategy for patients with claudin-low breast cancer.

Our work reveals novel SMO-independent activation of *GLI1* by the NFκB pathway, in which the p65 subunit of NFκB binds directly to the *GLI1* promoter in EMT and claudin-low cells (Figure 7C). We have only observed binding of the p65 subunit to one κB binding site in the *GLI1* promoter, but this does not preclude binding of NFκB subunits to the remaining putative κB binding sites in the *GLI1* promoter, perhaps following cytokine stimulation. Knockdown of NFκB subunits resulted in decreased *GLI1* expression (Figure 7D-E), indicating transcriptional regulation of *GLI1* by NFκB. *GLI1* levels were not completely abrogated following knockdown of NFκB subunits, indicating either that residual NFκB activity is sufficient to sustain *GLI1* expression, or that other pathways contribute to *GLI1* transcription.

We also found that NFκB is activated through a non-canonical pathway in EMT and claudin-low cells. Typically, in the absence of an inflammatory signal NFκB dimers are sequestered in the cytoplasm by IκBα. However, we observed NFκB in the nucleus of EMT and claudin-low cells (Figure 7A and Figure S5 in Additional file 1) without stimulation, indicating that NFκB is present in an activated form in the nucleus. Interestingly, we observed less nuclear NFκB in claudin-low cell lines, which express less *GLI1*, notably HS578T and MDA.MB.231 cells. This association fits with our data indicating transcriptional regulation of *GLI1* by NFκB, and speaks to the molecular heterogeneity of the claudin-low subclass. Indeed, while claudin-low tumors express more *GLI1* than the basal, human epidermal growth factor receptor 2 (Her2), and luminal B subtypes overall, there still existed heterogeneity within this subset (Figure 2D). Activated NFκB [53] and expression of *GLI1* [17-19] have been associated with poor prognosis in breast cancer. It will be interesting to see if NFκB activity and *GLI1* expression are correlated in mammary tumors. Recently, nuclear *GLI1* expression was shown to be closely correlated with nuclear expression of NFκB in pancreatic cancer, and both were associated with shorter overall survival and worse outcome [54]. It will be interesting to determine if a similar phenomenon occurs in breast cancer, and if patients with tumors that co-express NFκB and *GLI1* have a worse outcome.

Constitutive activation of NFκB in nuclear lysates from breast cancer cells has been observed [55], and it will be interesting to determine the responsible factors that contribute to NFκB pathway activation in EMT and claudin-low cells. One possibility is ERBB3, since recent work has revealed that the ERBB3 ligand heregulin increases mammosphere formation in breast cancer cell lines, which was attenuated by NFκB pathway inhibition [56]. It will be interesting to explore the role of ERBB3 on NFκB in claudin-low cells and EMT, especially given our findings with EGFR in EMT cells (Figure S1 in Additional file 1) and the known interactions among ERBB family members in breast cancer [57]. Recently Yamamoto *et al.* identified activated NFκB in basal and claudin-low tumors, and a correlation between NFκB activity and JAG1 expression, which was associated with poor prognosis in the basal subset [52]. These results combined with our findings suggest that NFκB could affect different downstream targets depending on subtype, namely JAG1 in basal and *GLI1* in claudin-low tumors.

Our work supports earlier studies implicating *GLI1* signaling in some breast cancer cell lines, albeit through different mechanisms. *GLI1* expression is elevated in SUM1315 cells, and knockdown of *GLI1* in MDA.MB.231 cells reduces cell growth, invasion, and metastasis [41].

Targeting *GLI1* in inflammatory breast cancer has been shown to decrease the migratory ability of these cells, and to increase apoptosis [38]. We have extended these findings to the claudin-low subtype as a class, and our findings lend evidence to the potential of *GLI1* as a therapeutic target in breast cancer.

There is increasing evidence for non-canonical Hh pathway activation in a variety of cancers [46] including breast [38,42]. Recently, Goel *et al.* demonstrated a contribution of Neuropilin-2 (*NRP2*), a vascular endothelial growth factor (VEGF) co-receptor, to *GLI1* levels in claudin-low cell lines [40]. A non-canonical mechanism was implicated, since *SMO* knockdown did not interfere with the process. It will be of interest to determine if *NRP2* exerts its effects on *GLI1* through NFκB. Although the NFκB and Hh pathways are implicated in breast cancer, and these pathways share some common downstream targets [58], to our knowledge direct transcriptional crosstalk between the two pathways in breast cancer has not yet been reported.

Although our studies focused on *GLI1*, *GLI2* expression is also elevated in EMT and claudin-low cells (Figure 2A-B). While *GLI1* is itself a *GLI1* regulatory target [34], in basal cell skin carcinoma cells, activation of *GLI2* by *GLI1* is indirect, and perhaps context dependent [59]. There are no consensus Gli or κB binding sites in the *GLI2* promoter. Therefore, it is likely that the regulation of *GLI2* expression in these cells occurs via a different mechanism than that described here for *GLI1*. Similarly, while some *GLI1* targets have been identified [37], the activity of the Gli proteins is highly context dependent [34], and it will be of great interest to determine the effectors through which Gli1 mediates the biological phenotypes we observed in claudin-low lines.

EMT cells and claudin-low cells are closely related to cancer stem cells [5-7]. There is evidence for Hh signaling in normal and malignant human mammary stem cells, and upregulation of *GLI1* in mammospheres [16]. We observed upregulation of *GLI1* in mammospheres, and a decrease in primary and secondary sphere formation after *GLI1* knockdown (Figure 5C), strongly suggesting a role for *GLI1* in maintenance of breast cancer stem cells/progenitor cells. Elevated levels of *GLI1* transcripts were also seen in a published dataset of mammospheres grown from primary patient material (Figure 2D). We have shown here evidence of crosstalk between the *GLI1* signaling and NFκB pathways in both EMT and claudin-low cell lines, indicating that activated *GLI1*, could be a mechanism that also operates in breast cancer stem cells. Recent reports substantiating the existence of cancer stem cells in solid tumors [60] reinforce the potential importance of these findings for breast cancer therapy.

## Conclusions

Several *SMO* antagonists are in clinical trials for the treatment of various cancers [61]. However, our findings indicate that, while bulk tumor and/or stromal cells may respond to *SMO* inhibitors, the tumor-initiating stem-like cells may not respond, possibly allowing for tumor resistance and recurrence. Crosstalk between these two key inflammatory and developmental pathways has important biological implications, and provides a rationale for combination therapy in the treatment of patients with claudin-low breast cancer. An increased molecular understanding of the signaling drivers in EMT and claudin-low cells may not only help patients with claudin-low or mesenchymal-like cancers, but could also aid in the prevention of metastasis and recurrence in breast cancer patients in general.

## Additional file

**Additional file 1: Table S1.** 150 compound screen. **Figure S1.** EMT cells have reduced EGFR and are resistant to EGFR inhibitors. **Figure S2.** *GLI2* and *GLI3* levels are not affected by JK184 treatment or by virus-expressing shGli1. **Figure S3.** Results of *GLI1* knockdown in control and basal cell lines. **Figure S4.** Biological replicate of *in vivo* experiment. **Figure S5.** Screen for upstream *GLI1* effectors. **Figure S6.** NFκB immunofluorescence in claudin-low cell lines. **Figure S7.** p65 ChIP from additional cell lines and additional knockdown experiments.

## Abbreviations

ANOVA: analysis of variance; BSA: bovine serum albumin; CDH1: E-cadherin; ChIP: chromatin immunoprecipitation; DCIS: ductal carcinomas *in situ*; EGFR: epidermal growth factor receptor; EMT: epithelial-to-mesenchymal transition; FBS: fetal bovine serum; GAPDH: glyceraldehyde phosphate dehydrogenase; *GLI1*: glioma-associated oncogene 1; *HER2*: human epidermal growth factor receptor 2; Hh: Hedgehog; HMLE: human mammary epithelial cells, transformed with large T and small t antigens; NFκB1: nuclear factor of kappa light polypeptide gene enhancer in B-cells 1; NFκB: nuclear factor kappa-light-chain-enhancer of activated B cells; *NRP2*: neuropilin-2; NT: non-targeting; PBS(T): phosphate-buffered saline (with 0.1% Tween-20); PCR: polymerase chain reaction; *PTCH1*: patched-1; *RELA*: v-rel reticuloendotheliosis viral oncogene homolog A; RT: room temperature; sh: short hairpin; *SMO*: smoothened; VEGF: vascular endothelial growth factor.

## Competing interests

The authors declare that they have no competing interests.

## Authors' contributions

SAC carried out and designed the experiments and drafted the manuscript. MRZ aided in conception and execution of the animal experiments. QY aided in the conception and design of the animal experiments. DXN analyzed published cell line expression data to create the gene expression heat map, made substantial contributions to the design of the experiments, and reviewed the manuscript critically for important intellectual content. DFS significantly contributed to the design and conception of the study, and critically reviewed the manuscript for intellectual content. All authors read and approved the final manuscript and agree to be accountable for the integrity of the work.

## Acknowledgements

We are grateful to Tisheeka Steed, Matthew Held, and the Yale Center for Molecular Discovery for assistance with the screen. We thank James Platt and Zongzhi Liu for help plotting and graphing results from the screen. We are grateful to Harriet Kluger, Yung-Chi Cheng, Gil Mor, A. Philip West, Seema Agarwal, and members of the Stern laboratory for helpful discussions and generous provision of some agents used in this work. We thank Robert A. Weinberg for supplying cell lines used in this study.



#### Grant support

This work was supported by PHS grant R01CA45708 awarded to D.F.S. S.A.C. is supported by grant #PF-13-082-01-TBE from the American Cancer Society. D.X.N. is a scholar of the V Foundation for Cancer Research, Yale Center for Clinical Investigation, and Young Investigator of the International Association for the Study of Lung Cancer. This work was supported in part by American Cancer Society Research Scholar Grant RSG-13-384-01-DMC awarded to Q. Y.

Received: 5 February 2014 Accepted: 8 September 2014

Published online: 25 September 2014

#### References

1. Sorlie T, Perou CM, Tibshirani R, Aas T, Geisler S, Johnsen H, Hastie T, Eisen MB, van de Rijn M, Jeffrey SS, Thorsen T, Quist H, Matese JC, Brown PO, Botstein D, Eystein Lonning P, Borresen-Dale AL: **Gene expression patterns of breast carcinomas distinguish tumor subclasses with clinical implications.** *Proc Natl Acad Sci U S A* 2001, **98**:10869–10874.
2. Network CGA: **Comprehensive molecular portraits of human breast tumours.** *Nature* 2012, **490**:61–70.
3. Perou CM: **Molecular stratification of triple-negative breast cancers.** *Oncologist* 2011, **16**:61–70.
4. Prat A, Adamo B, Cheang MC, Anders CK, Carey LA, Perou CM: **Molecular characterization of basal-like and non-basal-like triple-negative breast cancer.** *Oncologist* 2013, **18**:123–133.
5. Prat A, Parker JS, Karginova O, Fan C, Livasy C, Herschkowitz JI, He X, Perou CM: **Phenotypic and molecular characterization of the claudin-low intrinsic subtype of breast cancer.** *Breast Cancer Res* 2010, **12**:R68.
6. Lehmann BD, Bauer JA, Chen X, Sanders ME, Chakravarthy AB, Shyr Y, Pietenpol JA: **Identification of human triple-negative breast cancer subtypes and preclinical models for selection of targeted therapies.** *J Clin Invest* 2011, **121**:2750–2767.
7. Taube JH, Herschkowitz JI, Komurov K, Zhou AY, Gupta S, Yang J, Hartwell K, Onder TT, Gupta PB, Evans KW, Hollier BG, Ram PT, Lander ES, Rosen JM, Weinberg RA, Mani SA: **Core epithelial-to-mesenchymal transition interactome gene-expression signature is associated with claudin-low and metaplastic breast cancer subtypes.** *Proc Natl Acad Sci U S A* 2010, **107**:15449–15454.
8. Lee J, Platt KA, Censullo P, Ruiz i Altaba A: **Gli1 is a target of Sonic hedgehog that induces ventral neural tube development.** *Development* 1997, **124**:2537–2552.
9. Clement V, Sanchez P, de Tribolet N, Radovanovic I, Ruiz i Altaba A: **HEDGEHOG-GLI1 signaling regulates human glioma growth, cancer stem cell self-renewal, and tumorigenicity.** *Curr Biol* 2007, **17**:165–172.
10. Nesslering M, Richter K, Schwaenen C, Roerig P, Wrobel G, Wessendorf S, Fritz B, Bentz M, Sinn HP, Radlwimmer B, Lichter P: **Candidate genes in breast cancer revealed by microarray-based comparative genomic hybridization of archived tissue.** *Cancer Res* 2005, **65**:439–447.
11. Hu M, Yao J, Carroll DK, Weremowicz S, Chen H, Carrasco D, Richardson A, Violette S, Nikolskaya T, Nikolsky Y, Bauerlein EL, Hahn WC, Gelman RS, Allred C, Bissell MJ, Schnitt S, Polyak K: **Regulation of in situ to invasive breast carcinoma transition.** *Cancer Cell* 2008, **13**:394–406.
12. Wolf I, Bose S, Desmond JC, Lin BT, Williamson EA, Karlan BY, Koeffler HP: **Unmasking of epigenetically silenced genes reveals DNA promoter methylation and reduced expression of PTCH in breast cancer.** *Breast Cancer Res Treat* 2007, **105**:139–155.
13. Moraes RC, Zhang X, Harrington N, Fung JY, Wu M-F, Hilsenbeck SG, Allred DC, Lewis MT: **Constitutive activation of smoothened (SMO) in mammary glands of transgenic mice leads to increased proliferation, altered differentiation and ductal dysplasia.** *Development* 2007, **134**:1231–1242.
14. Vorechovsky I, Benediktsson KP, Toftgard R: **The patched/hedgehog/smoothened signalling pathway in human breast cancer: no evidence for H133Y SHH, PTCH and SMO mutations.** *Eur J Cancer* 1999, **35**:711–713.
15. Fiaschi M, Rozell B, Bergstrom A, Toftgard R: **Development of mammary tumors by conditional expression of GLI1.** *Cancer Res* 2009, **69**:4810–4817.
16. Liu S, Dontu G, Mantle ID, Patel S, Ahn NS, Jackson KW, Suri P, Wicha MS: **Hedgehog signaling and Bmi-1 regulate self-renewal of normal and malignant human mammary stem cells.** *Cancer Res* 2006, **66**:6063–6071.
17. Xu L, Kwon YJ, Frolova N, Steg AD, Yuan K, Johnson MR, Grizzle WE, Desmond RA, Frost AR: **Gli1 promotes cell survival and is predictive of a poor outcome in ERalpha-negative breast cancer.** *Breast Cancer Res Treat* 2010, **123**:59–71.
18. Ramaswamy B, Lu Y, Teng KY, Nuovo G, Li X, Shapiro CL, Majumder S: **Hedgehog signaling is a novel therapeutic target in tamoxifen-resistant breast cancer aberrantly activated by PI3K/AKT pathway.** *Cancer Res* 2012, **72**:5048–5059.
19. ten Haaf A, Bektas N, von Serenyi S, Losen I, Arweiler E, Hartmann A, Knuchel R, Dahl E: **Expression of the glioma-associated oncogene homolog (GLI) 1 in human breast cancer is associated with unfavourable overall survival.** *BMC Cancer* 2009, **9**:298.
20. Helbig G, Christopherson KW 2nd, Bhat-Nakshatri P, Kumar S, Kishimoto H, Miller KD, Broxmeyer HE, Nakshatri H: **NF-kappaB promotes breast cancer cell migration and metastasis by inducing the expression of the chemokine receptor CXCR4.** *J Biol Chem* 2003, **278**:21631–21638.
21. Gupta PB, Onder TT, Jiang G, Tao K, Kuperwasser C, Weinberg RA, Lander ES: **Identification of selective inhibitors of cancer stem cells by high-throughput screening.** *Cell* 2009, **138**:645–659.
22. Mani SA, Guo W, Liao MJ, Eaton EN, Ayyanan A, Zhou AY, Brooks M, Reinhard F, Zhang CC, Shipitsin M, Bauerlein EL, Hahn WC, Gelman RS, Allred C, Bissell MJ, Schnitt S, Polyak K: **The epithelial-mesenchymal transition generates cells with properties of stem cells.** *Cell* 2008, **133**:704–715.
23. Lu PJ, Sundquist K, Baekstrom D, Poulsom R, Hanby A, Meier-Ewert S, Jones T, Mitchell M, Pitha-Rowe P, Freemont P, Taylor-Papadimitriou J: **A novel gene (PLU-1) containing highly conserved putative DNA/chromatin binding motifs is specifically up-regulated in breast cancer.** *J Biol Chem* 1999, **274**:15633–15645.
24. Held MA, Langdon CG, Platt JT, Graham-Steed T, Liu Z, Chakraborty A, Bacchiocchi A, Koo A, Haskins JW, Bosenberg MW, Stern DF: **Genotype-selective combination therapies for melanoma identified by high-throughput drug screening.** *Canc Discov* 2013, **3**:52–67.
25. Varnat F, Duquet A, Malerba M, Zbinden M, Mas C, Gervaz P, Ruiz i Altaba A: **Human colon cancer epithelial cells harbour active HEDGEHOG-GLI signalling that is essential for tumour growth, recurrence, metastasis and stem cell survival and expansion.** *EMBO Mol Med* 2009, **1**:338–351.
26. Isohata N, Aoyagi K, Mabuchi T, Daiko H, Fukaya M, Ohta H, Ogawa K, Yoshida T, Sasaki H: **Hedgehog and epithelial-mesenchymal transition signaling in normal and malignant epithelial cells of the esophagus.** *Int J Cancer* 2009, **125**:1212–1221.
27. Lee UJ, Choung SR, Prakash KV, Lee EJ, Lee MY, Kim YJ, Han CW, Choi YC: **Dual knockdown of p65 and p50 subunits of NF-kappaB by siRNA inhibits the induction of inflammatory cytokines and significantly enhance apoptosis in human primary synovocytes treated with tumor necrosis factor-alpha.** *Mol Biol Rep* 2008, **35**:291–298.
28. Li YD, Ye BQ, Zheng SX, Wang JT, Wang JG, Chen M, Liu JG, Pei XH, Wang LJ, Lin ZX, Gupta K, Mackman N, Slungaard A, Key NS, Geng JG: **NF-kappaB transcription factor p50 critically regulates tissue factor in deep vein thrombosis.** *J Biol Chem* 2009, **284**:4473–4483.
29. Cheung WK, Zhao M, Liu Z, Stevens LE, Cao PD, Fang JE, Westbrook TF, Nguyen DX: **Control of alveolar differentiation by the lineage transcription factors GATA6 and HOPX inhibits lung adenocarcinoma metastasis.** *Cancer Cell* 2013, **23**:725–738.
30. Dontu G, Abdallah WM, Foley JM, Jackson KW, Clarke MF, Kawamura MJ, Wicha MS: **In vitro propagation and transcriptional profiling of human mammary stem/progenitor cells.** *Genes Dev* 2003, **17**:1253–1270.
31. O'Geen H, Frieze S, Farnham PJ: **Using ChIP-seq technology to identify targets of zinc finger transcription factors.** *Methods Mol Biol* 2010, **649**:437–455.
32. Tam WL, Lu H, Buikhuisen J, Soh BS, Lim E, Reinhardt F, Wu ZJ, Krall JA, Brierle B, Guo W, Chen X, Liu XS, Brown M, Lim B, Weinberg RA: **Protein kinase C alpha is a central signaling node and therapeutic target for breast cancer stem cells.** *Cancer Cell* 2013, **24**:347–364.
33. Lee J, Wu X, Pasca di Magliano M, Peters EC, Wang Y, Hong J, Hebrok M, Ding S, Cho CY, Schultz PG: **A small-molecule antagonist of the hedgehog signaling pathway.** *Chembiochem* 2007, **8**:1916–1919.
34. Stecca B, Ruiz IAA: **Context-dependent regulation of the GLI code in cancer by HEDGEHOG and non-HEDGEHOG signals.** *J Mol Cell Biol* 2010, **2**:84–95.
35. Neve RM, Chin K, Fridlyand J, Yeh J, Baehner FL, Fevr T, Clark L, Bayani N, Coppe JP, Tong F, Speed T, Spellman PT, DeVries S, Lapuk A, Wang NJ, Kuo WL, Stilwell JL, Pinkel D, Albertson DG, Waldman FM, McCormick F, Dickson RB, Johnson MD, Lippman M, Ethier S, Gazdar A, Gray JW: **A collection of breast cancer cell lines for the study of functionally distinct cancer subtypes.** *Cancer Cell* 2006, **10**:515–527.

36. Prat A, Karginova O, Parker JS, Fan C, He X, Bixby L, Harrell JC, Roman E, Adamo B, Troester M, Perou CM: **Characterization of cell lines derived from breast cancers and normal mammary tissues for the study of the intrinsic molecular subtypes.** *Breast Cancer Res Treat* 2013, **142**:237–255.
37. Yoon JW, Kita Y, Frank DJ, Majewski RR, Konicek BA, Nobrega MA, Jacob H, Walterhouse D, Iannaccone P: **Gene expression profiling leads to identification of GLI1-binding elements in target genes and a role for multiple downstream pathways in GLI1-induced cell transformation.** *J Biol Chem* 2002, **277**:5548–5555.
38. Thomas ZI, Gibson W, Sexton JZ, Aird KM, Ingram SM, Aldrich A, Lysterly HK, Devi GR, Williams KP: **Targeting GLI1 expression in human inflammatory breast cancer cells enhances apoptosis and attenuates migration.** *Br J Cancer* 2011, **104**:1575–1586.
39. Tate CR, Rhodes LV, Segar HC, Driver JL, Pounder FN, Burrow ME, Collins-Burrow BM: **Targeting triple-negative breast cancer cells with the histone deacetylase inhibitor panobinostat.** *Breast Cancer Res* 2012, **14**:R79.
40. Goel HL, Pursell B, Chang C, Shaw LM, Mao J, Simin K, Kumar P, Vander Kooi CW, Shultz LD, Greiner DL, Norum JH, Toftgard R, Kuperwasser C, Mercurio AM: **GLI1 regulates a novel neuropilin-2/alpha6beta1 integrin based autocrine pathway that contributes to breast cancer initiation.** *EMBO Mol Med* 2013, **5**:488–508.
41. Kwon YJ, Hurst DR, Steg AD, Yuan K, Vaidya KS, Welch DR, Frost AR: **Gli1 enhances migration and invasion via up-regulation of MMP-11 and promotes metastasis in ERalpha negative breast cancer cell lines.** *Clin Exp Metastasis* 2011, **28**:437–449.
42. Zhang X, Harrington N, Moraes RC, Wu MF, Hilsenbeck SG, Lewis MT: **Cyclopamine inhibition of human breast cancer cell growth independent of Smoothened (Smo).** *Breast Cancer Res Treat* 2009, **115**:505–521.
43. Seto M, Ohta M, Asaoka Y, Ikenoue T, Tada M, Miyabayashi K, Mohri D, Tanaka Y, Ijichi H, Tateishi K, Kanai F, Kawabe T, Omata M: **Regulation of the hedgehog signaling by the mitogen-activated protein kinase cascade in gastric cancer.** *Mol Carcinog* 2009, **48**:703–712.
44. Katoh Y, Katoh M: **Integrative genomic analyses on GLI1: positive regulation of GLI1 by Hedgehog-GLI, TGFbeta-Smads, and RTK-PI3K-AKT signals, and negative regulation of GLI1 by Notch-CSL-HES/HEY, and GPCR-Gs-PAK signals.** *Int J Oncol* 2009, **35**:187–192.
45. Nolan-Stevaux O, Lau J, Truitt ML, Chu GC, Hebrok M, Fernandez-Zapico ME, Hanahan D: **GLI1 is regulated through Smoothened-independent mechanisms in neoplastic pancreatic ducts and mediates PDAC cell survival and transformation.** *Genes Dev* 2009, **23**:24–36.
46. Wang Y, Ding Q, Yen C, Xia W, Izzo J, Lang JY, Li CW, Hsu JL, Miller SA, Wang X, Lee DF, Hsu JM, Huo L, Labaff AM, Liu D, Huang TH, Lai CC, Tsai FJ, Chang WC, Chen CH, Wu TT, Buttar NS, Wang KK, Wu Y, Wang H, Ajani J, Hung MC: **The crosstalk of mTOR/S6K1 and Hedgehog pathways.** *Cancer Cell* 2012, **21**:374–387.
47. Jang BC, Lim KJ, Choi IH, Suh MH, Park JG, Mun KC, Bae JH, Shin DH, Suh SI: **Triptolide suppresses interleukin-1beta-induced human beta-defensin-2 mRNA expression through inhibition of transcriptional activation of NF-kappaB in A549 cells.** *Int J Mol Med* 2007, **19**:757–763.
48. Kim YH, Lee SH, Lee JY, Choi SW, Park JW, Kwon TK: **Triptolide inhibits murine-inducible nitric oxide synthase expression by down-regulating lipopolysaccharide-induced activity of nuclear factor-kappa B and c-Jun NH2-terminal kinase.** *Eur J Pharmacol* 2004, **494**:1–9.
49. Qiu D, Zhao G, Aoki Y, Shi L, Uyei A, Nazarian S, Ng JC, Kao PN: **Immunosuppressant PG490 (triptolide) inhibits T-cell interleukin-2 expression at the level of purine-box/nuclear factor of activated T-cells and NF-kappaB transcriptional activation.** *J Biol Chem* 1999, **274**:13443–13450.
50. Bhat-Nakshatri P, Sweeney CJ, Nakshatri H: **Identification of signal transduction pathways involved in constitutive NF-kappaB activation in breast cancer cells.** *Oncogene* 2002, **21**:2066–2078.
51. Sovak MA, Bellas RE, Kim DW, Zarnieski GJ, Rogers AE, Traish AM, Sonenshein GE: **Aberrant nuclear factor-kappaB/Rel expression and the pathogenesis of breast cancer.** *J Clin Invest* 1997, **100**:2952–2960.
52. Yamamoto M, Taguchi Y, Ito-Kureha T, Semba K, Yamaguchi N, Inoue J: **NF-kappaB non-cell-autonomously regulates cancer stem cell populations in the basal-like breast cancer subtype.** *Nat Commun* 2013, **4**:2299.
53. Ingles-Esteve J, Morales M, Dalmases A, Garcia-Carbonell R, Jene-Sanz A, Lopez-Bigas N, Iglesias M, Ruiz-Herguido C, Rovira A, Rojo F, Albanell J, Gomis RR, Bigas A, Espinosa L: **Inhibition of specific NF-kB activity contributes to the tumor suppressor function of 14-3-3σ in breast cancer.** *PLoS One* 2012, **7**:e38347.
54. Yang SH, Hsu CH, Lee JC, Tien YW, Kuo SH, Cheng AL: **Nuclear expression of glioma-associated oncogene homolog 1 and nuclear factor-kappaB is associated with a poor prognosis of pancreatic cancer.** *Oncology* 2013, **85**:86–94.
55. Nakshatri H, Bhat-Nakshatri P, Martin DA, Goulet RJ Jr, Sledge GW Jr: **Constitutive activation of NF-kappaB during progression of breast cancer to hormone-independent growth.** *Mol Cell Biol* 1997, **17**:3629–3639.
56. Hinohara K, Kobayashi S, Kanauchi H, Shimizu S, Nishioka K, Tsuji E, Tada K, Umezawa K, Mori M, Ogawa T, Inoue J, Tojo A, Gotoh N: **ErbB receptor tyrosine kinase/NF-kappaB signaling controls mammosphere formation in human breast cancer.** *Proc Natl Acad Sci U S A* 2012, **109**:6584–6589.
57. Stern DF: **Tyrosine kinase signalling in breast cancer: ErbB family receptor tyrosine kinases.** *Breast Cancer Res* 2000, **2**:176–183.
58. Katoh M: **Integrative genomic analyses of ZEB2: transcriptional regulation of ZEB2 based on SMADs, ETS1, HIF1alpha, POU/OCT, and NF-kappaB.** *Int J Oncol* 2009, **34**:1737–1742.
59. Regl G, Neill GW, Eichberger T, Kasper M, Ikram MS, Koller J, Hintner H, Quinn AG, Frischauf AM, Aberger F: **Human GLI2 and GLI1 are part of a positive feedback mechanism in basal cell carcinoma.** *Oncogene* 2002, **21**:5529–5539.
60. Driessens G, Beck B, Caauwe A, Simons BD, Blanpain C: **Defining the mode of tumour growth by clonal analysis.** *Nature* 2012, **488**:527–530.
61. Ng JM, Curran T: **The Hedgehog's tale: developing strategies for targeting cancer.** *Nat Rev Cancer* 2011, **11**:493–501.

doi:10.1186/s13058-014-0444-4

**Cite this article as:** Colavito et al.: Significance of glioma-associated oncogene homolog 1 (GLI1) expression in claudin-low breast cancer and crosstalk with the nuclear factor kappa-light-chain-enhancer of activated B cells (NFkB) pathway. *Breast Cancer Research* 2014 **16**:444.

**Submit your next manuscript to BioMed Central and take full advantage of:**

- Convenient online submission
- Thorough peer review
- No space constraints or color figure charges
- Immediate publication on acceptance
- Inclusion in PubMed, CAS, Scopus and Google Scholar
- Research which is freely available for redistribution

Submit your manuscript at  
www.biomedcentral.com/submit

